SIMULATION AND DESIGN METHOD IN ADVANCED NANOMATERIALS FINE-TUNING FOR SOME PEROVSKITES TYPE AHE STUDY

S. MOHORIANU, M. LOZOVAN, F.-V. RUSU

National Institute of Research and Development for Technical Physics – IFT Iaşi, 47 Mangeron Blvd. 700050, Iaşi, Romania,
E-mail: sergium@phys-iasi.ro

Received January 25, 2008

Nanostructured materials with tailored properties are now essential for future applications in the current industrial manufacturing. Extracting valuable information from data by using the distributed computer processing and storage technologies, as well the Artificial Neural Network (ANN) and the development of advanced algorithms for knowledge discovery are the purpose of our work. We describe how a Simulation and Design Method (SDM) attempt, based on our last results, is applied on two perovskites type materials, $La_{0.7}Ca_{0.3}MnO_3$ and $La_{0.7}Sr_{0.3}MnO_3$ in order to study the Anomalous Hall Effect (AHE). Our new ANN model, is intended to contribute to the effort to improve some properties of new materials. It implements and uses the basic building blocks of neural computation, such as multi-layer perceptrons. ANN can learn associative patterns and approximate the functional relationship between a set of input and output. Modeling and simulation techniques affect all stages in the development and improvement of new materials, from the initial formation of concepts to synthesis and characterization of properties. A new SDM with ANN for some nanomagnetic materials was given. Neural networks have been applied successfully in the identification and classification of some nanomagnetic characteristics from a large amount of data.

Key words: LCMO, LSMO, perovskite structure, AHE, GMR, ANN.

1. INTRODUCTION

Nanostructured materials that have tailored properties to achieve improved mechanical, electrical, optical, magnetic and other functional properties are now essential for future applications in the current industrial manufacturing. Currently nanomagnetism research involves investigating the basic magnetic, magneto-optical, galvanomagnetic, magnetotransport phenomena associated with reduced dimensionality. As a result a lot of data emerge. The idea of extracting valuable information from data, *data mining*, is not new [1]. New is the distributed computer processing and storage technologies, which allow gigabytes, even terabytes of data to

remain on-line, available for processing by client/server applications. It's new as well, the Artificial Neural Network (ANN) use and the development of advanced algorithms for knowledge discovery. The continuous evolution in the actual technology of nanomaterials requires a careful understanding of physical and chemical properties of materials, structures and processes at the micro- and nanoscale. The major research objectives in advanced nanostructured and multifunctional materials are still the modeling and design, the characterization and the fabrication of useful functional materials.

Magnetotransport in mixed-valent manganese oxides with perovskite structure in heterogeneous, layered or granular metallic systems is a recent subject of interest [2], because of the significant reduction in the electrical resistance when a magnetic field is applied. The Hall Effect becomes **A**nomalous **H**all **E**ffect (AHE). Generally speaking, the Hall resistivity ρ_{xy} of a magnetic metal may be expressed in terms of two contributions: $\rho_{xy} = R_0 B + R_S(\mu_0 M)$, where $R_0 = 1/(ne)$ is the Hall coefficient due to the Lorentz force on the conducting carriers of a density n and electric charge e, $\boldsymbol{B}$ is the magnetic induction, and Rs is the anomalous Hall coefficient associated with the magnetization $\boldsymbol{M}$ of the sample. Theory attributes the AHE to the asymmetric (skew) scattering of carriers relative to the plane spanned by $\boldsymbol{M}$ and the electrical current, or to the side-jump mechanism, mechanisms due to the spin-orbit interaction. Recent studies [3–5] have focused on the Hall Effect in the family of doped manganese oxides $La_{1-x}A_xMnO_3$ (in which A stands for Ca, Sr or Pb), famous for its Colossal MagnetoResistance (CMR) and accompanying ferromagnet-to-paramagnet (FP) and metal-insulator (MI) transitions. Since the magnetic behavior of nanomaterials is still largely unknown, much of the focus in this effort is directed toward measuring the magnetic characteristics of this class of materials and checking if they are consistent with present theories explaining the behavior of conventional materials. The atomic structure of nanostructured materials is different than that seen in crystals or glasses because of the large volume fraction *>50%* of grain boundaries or interfaces. Nanometer sized materials (*1* to *100 nm*) contain about 900 atoms if zero-dimensional shape nanomaterial is considered. The magnetic permeability, the magnetic anisotropy, the electrical conductivity are strong and effectively correlated with: *i)* the chemical composition, *ii)* the material structure and *iii)* grain size of the nanomagnetic material [6, 7].

Microscopic theory of AHE has been of long debate for half a century, and is being developed quite recently to explain AHE in various ferromagnetic metals quantitatively, in which the *Berry phase* of *Bloch wave function* plays a decisive role. For general consideration of AHE, more comprehensive treatment is needed

than the well known skew scattering and side jump mechanisms. In a recent theory for multiband ferromagnetic metals with dilute impurities, the power law dependence of the anomalous Hall conductivity σ_{AH} on the conductivity σ_{xx} was shown to have an extrinsic-to intrinsic crossover with different exponents at a certain value of conductivity, $\sigma_{AH} \propto \sigma_{xx}$.

2. THE MODEL AND THE SIMULATION

In this work a back-propagation based on an ANN method is used. We describe how a **S**imulation and **D**esign **M**ethod (SDM) attempt based on our last results [8, 9], is applied on two perovskites type materials, $La_{0.7}Ca_{0.3}MnO_3$ (LCMO) and $La_{0.7}Sr_{0.3}MnO_3$ (LSMO) respectively, in order to study the Anomalous Hall Effect (AHE).

2.1. MODELING INSTRUMENT DESCRIPTION

On the global framework of computational nanotechnology [10] it clearly appears that the software required for the modeling and to design complex molecular structures becomes progressively available.

An Artificial Neural Network (ANN) is a simulation of the functioning of the human nervous system that produces the required response to input. ANN is able to provide some of the human characteristics of problem-solving ability that are difficult to simulate using logical, analytical techniques. One of the advantages of using ANN is that it doesn't need a predefined knowledge base. ANN can learn associative patterns and approximate the functional relationship between a set of input and output. A well-trained ANN, for example, may be able to discern, with a high degree of consistency, patterns that human experts would miss. In a neural network, the fundamental variables are the set of connection weights. A network is highly interconnected and consists of many neurons that perform parallel computations. Each neuron is linked to other neurons with varying coefficients of connectivity that represent the weights of these connections. Learning by the network is accomplished by adjusting these weights to produce appropriate output through training examples feed to the network. The multilayer perceptron (MLP) is one of the most widely implemented neural network topologies. Generally speaking, for static pattern classification, the MLP with two hidden layers is a universal pattern classifier.

Our new ANN model is intended to contribute on this effort and to improve some properties of the new materials. This new method requires a large amount of data; some of them direct measurable, collected from experiences made using different substances and materials with magnetic properties. We use both data from our laboratory and data already published. Unlike more analytically based

information processing methods, neural computation effectively explores the information contained within input data, without further assumptions. The methods are based on assumptions about input data ensembles.

Artificial intelligence encodes a prior human knowledge with simple *if-then* rules, performing inference on these rules to reach a conclusion [11]. With Neural Networks, we can *discover* relationships in the input data sets through the iterative presentation of the data using the intrinsic mapping characteristics of neural topologies – *learning*. There are two basic phases in a neural network operation. The *training* phase, where data is repeatedly presented to the network, while its weights are updated to obtain a desired response; and the recall or *retrieval phase*, where the trained network with frozen weights is applied to new data, which were never seen. The learning phase is time consuming due to the iterative nature of searching for the best performance. Once the network was trained, the retrieval phase can be very fast, because processing can be distributed. In our recent SDM attempt Neural Networks were used for both, regression and classification. In *regression* the outputs represent some desired, continuously valued transformation of the input patterns. In *classification*, the objective is to assign the input patterns to one of several categories or classes, usually represented by outputs restricted to lie in the range from *0* to *1*, so that they represent the probability of class membership. For regression, it can be shown that a single hidden layer Multilayer Perceptron (MLP) can learn any desired continuous input-output mapping if there are sufficient numbers of axons in the hidden layer(s). For classification, MultiLayer Perceptrons (MLP) can learn the Bayesian posterior probability of correct classification. This means that the Neural Network takes into account the relative frequency of occurrence of the classes, giving more weight to frequently occurring classes. Neural Networks have been trained to perform this complex functions for *identification* and *classification*.

2.2. EXPERIMENTAL DATA AND THE SIMULATION

As it results from a large number of experimental data [2], [4] devoted to the AHE study for some itinerant ferromagnets, ferromagnetic semiconductors and metals, one can see a σ_{AH} dependence on σ_{xx} (the scaling relation) as composition vary, see Table 1. *(La,A)MnO₃* is usually ferromagnetic metal with double exchange mechanism, where alkaline-earth element serves as hole dopants. The content *A* affects also the magnetic phases. For *(La,A)MnO₃* the scaling relation is nearly extrapolated from *(Ti,Co)O₂* .

New experimental observations provide data that indicate a strong correlation between the thickness of epitaxial films and the corresponding magnetoresistance; other indicate that an increasing of lattice distortion by the substitution of *La* ions by smaller ions (*Y i.e.)* present a decreasing of T_C , Curie temperature and an increasing of CMR.

At room temperature LCMO present an orthorhombic structure (space group *Pnma*) with lattice parameters $a \approx \sqrt{2}a_p$, $b \approx 2a_p$, $c \approx \sqrt{2}a_p$ where a_p is the lattice parameter of a simple cubic perovskite. The long orthorhombic *b* axis can be directed along any one of the cubic axis. The *a* and *c* orthorhombic axes are perpendicular to *b* and rotated 45° with respect to the cubic axes. Depending on the direction of the *b* axis with respect to the cubic cell, three different orientations of the *Pnma* unit cell are possible. Within each orientation *a* and *c* axis can be interchanged, leading to additional pair of twins.

Domains with mutually perpendicular *b* axes, refereed to as orthogonal twins, are preferentially separated by {110} cubic planes. Twins with common *b* axis but with different *a* and *c* axis, so-called permutation twins, are separated by {100} cubic planes.

Table 1

A list of ferromagnetic semiconductors and metals. The measured temperature (*T*), the Curie temperature (T_c), the conduction states, and the scaling relation (a- and r- denote anatase and rutile TiO_2)

Composition	*T(K)*	T_C*(K)*	Conduction states	$\sigma_{AH} \propto \sigma_{xx}$ scaling relation	Ref.
r-$Ti_{1-x}Co_xO_2$	100–300	>400	hopping		[12]
r-$Ti_{0.98}Co_{0.02}O_2$	200–300	>400	hopping	$\sigma_{AH} \propto \sigma_{xx}^{1.5-1.7}$	[13]
a-$Ti_{0.95}Co_{0.05}O_2$		>400	metallic		[14]
a-$Ti_{0.92}Co_{0.05}Nb_{0.03}O_2$		>400	metallic		[15]
$Ga_{0.947}Mn_{0.053}As$	2–150	110	metallic		[16]
$Ga_{0.94}Mn_{0.06}As$	0.4	132	metallic		[17]
$Ga_{0.915}Mn_{0.085}As$	10–60	0–30	hopping		[18]
$Ga_{1-x}Mn_xAs$	10–160	120–145	metallic	$\sigma_{AH} \propto \sigma_{xx}^{1.6}$	[19]
$In_{0.987}Mn_{0.013}As$	3.5	7.5	hopping		[20]
$In_{1-x}Mn_xAs$	4.2	35	metallic		[21]
$Ga_{0.977}Mn_{0.023}Sb$	1.5–30	25	metallic		[22]
$In_{0.98}Mn_{0.02}Sb$	1.5–12	7	metallic		[23]
$La_{0.7}Ca_{0.3}MnO_3$	10–300	216	metallic		[24]
$La_{0.7}Ca_{0.3}MnO_3$	250–320	265	metallic		[25]
$La_{0.67}(Ca,Pb)_{0.33}MnO_3$	100–350	285	metallic	$\sigma_{AH} \propto \sigma_{xx}^{1.5}$	[24]
$La_{0.7}Sr_{0.3}MnO_3$	10–400	362	metallic		[24]
$La_{1-x}Sr_xCoO_3$	40–300	120–230	hopping, metallic		[26]
$SrRuO_3$ (single crystal)	–	160	metallic		[4]
$Sr_{1-x}Ca_xRuO_3$	2–160	70–150	metallic		[27]
Sr_2FeMoO_6	5	420	metallic	$\sigma_{AH} \propto \sigma_{xx}$	[28]
$Nd_2Mo_2O_7$	2–100	89	metallic		[29]
$Fe_{1-x}Mn_xSi$	5	0–30	metallic		[30]
$Fe_{1-x}Co_xSi$	5	10–47	metallic		[30]

To overcome the difficulties arising from a manual assisted procedure, a back-propagation algorithm is used. *What we expect from our new method?* Since ANN learns from the data, the data must be valid for the results to be meaningful. Sometimes the desired response is unknown. Our model implements and uses the basic building blocks of neural computation, such as multi-layer perceptrons (MLP). In our actual work we use **NeuroSolutions**, a ***Neuro Dimension Inc.*** product. A successful Neural Network simulation requires the specification of many parameters. The performance is highly dependent on the accurate choice of these parameters.

Assume that d is a function of several inputs $x_1, x_2, ..., x_D$, independent variables, and the goal is to find the best linear regressor of d on all the inputs, Figure 1.

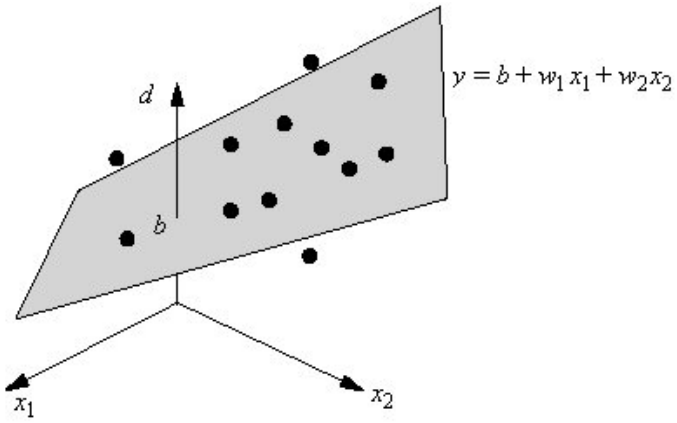

Fig. 1. – The concept representation of the multilinear regression.

For $D = 2$ this corresponds to fitting a plane through the N input samples or a hyperplane in the general case of D dimensions. As an example, let us assume that we have two variables x_1 ($B(T)$ – the magnetic field induction) and x_2 (I (mA) – the current through the probe) that affect the anomalous Hall voltage ($d \equiv U_{AH}(\mu V)$) achieved. In normalized abstract units, the values [31] of x_1, x_2, d are presented in Table 2.

Table 2

The dependent and the independent variable

x_1 ($B/10$)	($d \equiv U_{AH}$)			
	Composition			
	$La_{0.7}Ca_{0.3}MnO_3$		$La_{0.7}Sr_{0.3}MnO_3$	
	x_2	d	x_2	d
0	10	0	15	0
1	10	40	15	10
2	10	100	15	20
6	10	300	15	40

8	10	550	15	60
10	10	920	15	70
13	10	1200	15	85
14	10	1400	15	90
15	10	1550	15	95
15.5	10	1650	15	97
16	10	1750	15	98
16.5	10	1830	15	98
17.5	10	1950	15	99
18	10	2000	15	100

The goal is to find how well one can explain the quality of d by the two variables x_1, and x_2, and which is the most important parameter. We assume that the measurements x, are noise free and that d is contaminated by a noise vector ε with these properties: Gaussian distributed with components that are zero mean, of equal variance σ^2, and uncorrelated with the inputs. The regression equation when $D = 2$, looks as follow:

$$\varepsilon_i = d_i - (b + w_1 x_{i1} + w_2 x_{i2}) \tag{1}$$

where x_{1i} is the ith value of x_1. In the general case we write (eq. 1) as:

$$\varepsilon_i = d_i - \left(b + \sum_{k=1}^{D} w_k x_{ik} \right) = d_i - \sum_{k=0}^{D} w_k x_{ik} \qquad i = 1...N \tag{2}$$

where we made $w_0 = b$ and $x_{i0} = 1$. The goal of the regression problem is to find the coefficients $w_0,...,w_D$. To simplify the notation we will put all these values into a vector $w = \left[w_0,...,w_D \right]^T$ that minimizes the MSE (Mean Square Error) of ε_i over the N samples.

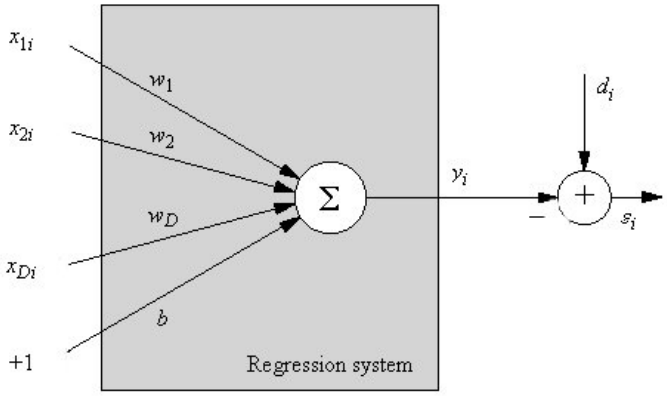

Fig. 2. – The linear Processing Element.

Figure 2 show that the linear Processing Element (PE) has D inputs and one bias. We have created the multiple linear regression breadboards. For multiple

regressions, we simply change the input file and desired file to ASCII files which contain data from a more complex table.

The network is the same, except since there are more inputs, the input axon has more elements (one for each input, although the icon is exactly the same) each of which is connected to a single bias axon. This means that the synapse now has more weights (one for each input). Everything else is exactly the same except that the "input and regression line" plot has no longer meaning. If we use the autocorrelation matrix for the data, then solve for the eigenvalues, we find the eigenvalues are 59 and 1.5, giving us an eigenvalue spread of roughly 40. This produces a very skewed (much narrower in one direction) performance surface. We run the network with a learning rate of 0.005 and we notice that there is a very quick drop in the MSE followed by a very slow descent in the learning curve. This is because the performance surface is much steeper in one direction than in the other.

3. RESULTS AND DISCUSSION

One of the advantages of using ANN is that it doesn't need a predefined knowledge base. ANN can learn associative patterns and approximate the functional relationship between a set of input and output. A well-trained ANN, may be able to discern, with a high degree of consistency, patterns that human experts would miss. In a Neural Network, the fundamental variables are the set of connection weights. The MLPs are trained with error correction learning, which means that the desired response for the system must be known, as well known as back propagation algorithm.

When we run the network, we see that the learning curve (one of our only indications of whether the network is training correctly), decreases steadily and that the weights eventually approach the theoretical optimal weights. The remarkable thing about the adaptive system's methodology is that if we changed the problem, the technique to solve did not change significantly. It is true that we have to redimension the system properly and choose new values for the step size, but the fundamental aspects of the methodology did not change at all.

3.1. THE PREDICTED OUTPUT AND THE KNOWN OUTPUT

An MLP for back-propagation type neural network model was operate (Fig. 3) in this work using NeuroSolutions 4.10 software (NeuroDimension, 2004).

The architecture of the network consists of (a) *one input layer that contains 7 input variables*, (b) *one hidden layer of 5 nodes*, (c) *one output layer that contains 1 output variable*, and (d) *connection weights that connect all layers*

together (see figure 3). User interaction with NeuroSolutions follows very simple and clear principles:

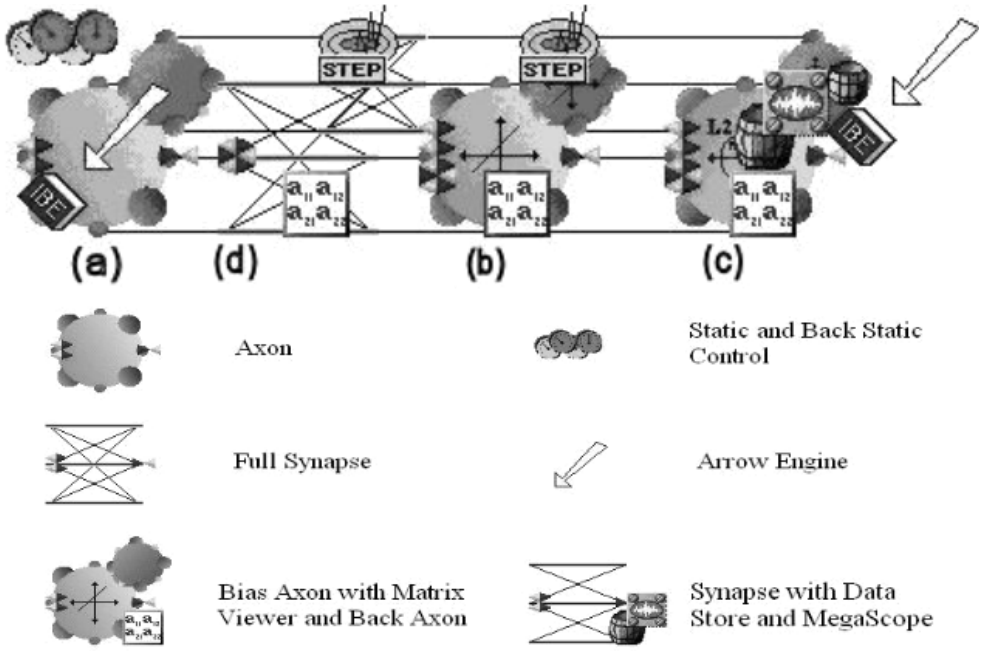

Fig. 3. – The ANN selected to solve the SDM fine-tuning.

1. Each neural component is represented by an icon.
2. A component's inspector is where the user can inspect and alter any variables of the component.
3. Animation windows allow components to display data while a simulation is running.
4. Networks are constructed by placing and interconnecting components on a breadboard.
5. Components are created by selecting them from palettes and stamping them onto the breadboard. Components can be removed from the topology by means of the cut operation.

In Figure 3 some of the principal ANN elementary graphic interfaces used are nominated.

There are two important parameters including a learning rate coefficient (Eta) and a momentum factor (Alpha) during training. In general, Eta's valid range is between 0.0 and 1.0. We change the learning rate to various values and watch the network learning. We found an optimal learning rate of 0.005 (see an intermediate state in Fig. 4).

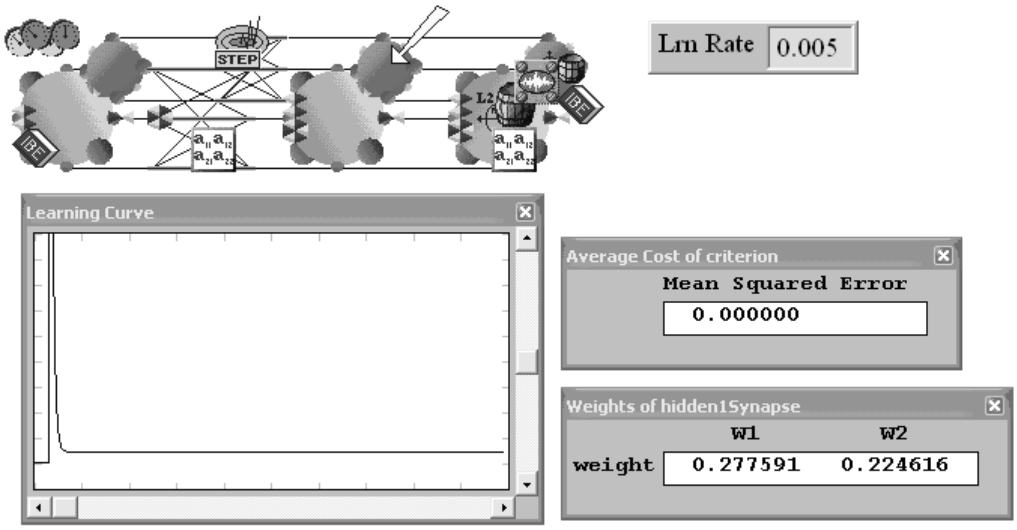

Fig. 4. – The runing Neural Network with initial learning rate.

We notice that after 300 iterations, the network weights estimated allow the solution to come close to the experimental [31] known solution, as shown in Fig. 5.

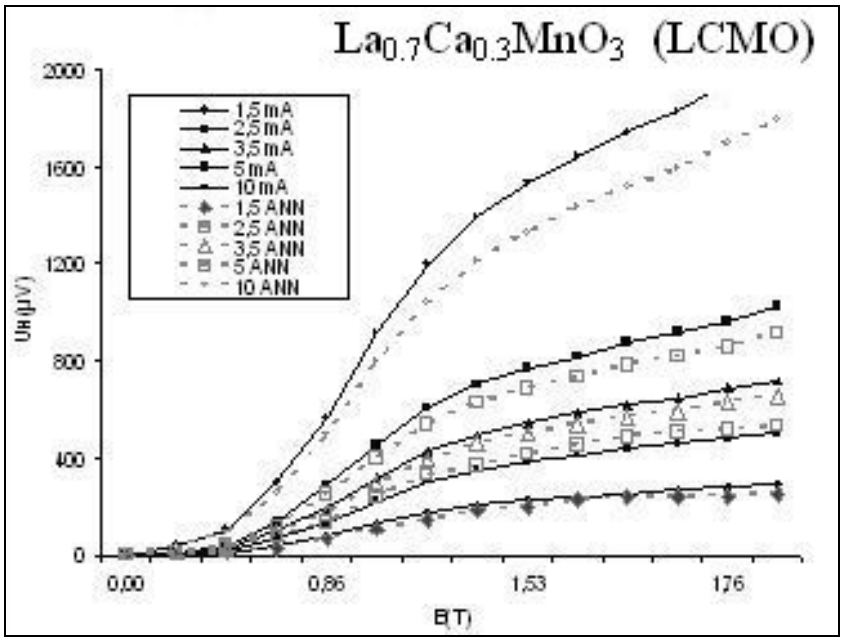

Fig. 5. – The two types of data for $La_{0.7}Ca_{0.3}MnO_3$:
Experimental data *(line)*; Simulated data with ANN *(doted line)*.

4. CONCLUSIONS

Low dimensional magnetic systems, such as thin films, multilayers, and surfaces exhibit many scientifically interesting and technologically useful properties.

Modeling has now a very important position in the development and improvement of new materials for applications. Modeling and simulation techniques affect all stages in the development and improvement of new materials, from the initial formation of concepts to synthesis and characterization of properties. A new SDM with ANN for some nano-magnetic materials was given. Neural networks have been applied successfully in the identification and classification of some nanomagnetic characteristics from a large amount of data. The universal approximation capabilities of the multilayer perceptron make it a useful choice for modeling nonlinear systems and for implementing general-purpose controllers and magnetic characteristics extractor from wide data amount.

The Hall Effect in magnetic metals consists of two parts. One is due to the Lorentz force. The other, extraordinary contribution – originates from asymmetry of magnetic scattering and is thus proportional to magnetization, as well as a power of resistivity. The magnetic domain topology of the $La_{0.78}$ $Ca_{0.22}$ MnO_3 crystals is correlated with the intrinsic twin structure. In the temperature range 70–150 K significant changes in apparent rotation of the domain walls was found. With the temperature decreasing the regular network of ferromagnetic domains undergo. The apparent rotation of the domain walls can be understood in terms of the Jahn-Teller deformation of the orthorhombic unit cell, accompanied by additional twinning.

Our SDM permit the search of the correlation for new materials properties and to enhance actual magnetic properties. Our simulation with ANN is in good concordance with experimental data.

REFERENCES

1. J.P. Bigus, Data Mining with Neural Networks, McGraw-Hill, 1996.
2. T. Fukumura, H. Ttoyosaki, K. Ueno, M. Nakano, T. Yamasaki, M. Kawasaki, Japanese Journal of Applied Physics Vol. **46**, No. 26, L642–L644, (2007).
3. A.V. Samoilov, G. Beach, C.C. Fu and N.-C. Yeh, R.P. Vasquez, *Magnetic percolation and giant spontaneous Hall effect in* $La_{1-x}Ca_xCoO_3$ *(0.2<x<0.5)*, Physical Review B, Volume **57**, Number 22, June (1998).
4. T. Miyasato, N. Abe, T. Fujii, A. Asamitsu, S. Onoda, Y. Onose, N. Nagaosa, Y. Tokura, *Universal Scaling Behavior of Anomalous Hall Effect and Anomalous Nernst Effect in Itinerant Ferromagnets*, http://arXiv:cond-mat/0610324 v1.
5. J. Ivcov, *The Hall effect in amorphous alloys of early and late transition metals*, Fizika *A4* 3, 561–570 (1995).
6. T. Zhang, G. Li, T. Qian, J.F. Qu, X.Q. Xiang, X.G. Li, *Effect of particle size on the structure and magnetic properties of La0.6Pb0.4MnO3 nanoparticles*, Journal of Applied Physics **100**, 094324, (2006).
7. Jagdish Narayan, *Critical size for defects in nanostructured materials*, Journal of Applied Physics **100**, 034309, (2006).

8. S. Mohorianu, M. Lozovan, *Rom. Journ. Phys.,* Vol. **52**, Nos. 3–4*,* 337 (2007).
9. S. Mohorianu, M. Lozovan, C. Baciu, JOAM, Vol. **9**, No. 5, p. 1499–1504, May (2007).
10. R.C. Merkle, *Computational nanotechnology*, Nanotechnology, vol. **2,** p. 134 (1991).
11. M.A. Arbib – editor: *The Handbook of Brain Theory and Neural Networks* – Second Edition, the MIT Press, Cambridge – Massachusetts, London – England, 2003.
12. H. Toyosaki, T. Fukumura, Y. Yamada, K. Nakajima, T. Chikyow, T. Hasegawa, H. Koinuma, and M. Kawasaki: Nat. Mater. **3** (2004) 221.
13. J.S. Higgins, S.R. Shinde, S.B. Ogale, T. Venkatesan, R.L. Greene, Phys. Rev. B **69** (2004) 073201.
14. K. Ueno, T. Fukumura, H. Toyosaki, M. Nakano, M. Kawasaki, Appl. Phys. Lett. **90** (2007) 072103.
15. T. Hitosugi, G. Kinoda, Y. Yamamoto, Y. Furubayashi, K. Inaba, Y. Hirose, K. Nakajima, T. Chikyow, T. Shimada, T. Hasegawa, J. Appl. Phys. **99** (2006) 08M121.
16. F. Matsukura, H. Ohno, A. Shen, Y. Sugawara, Phys. Rev. B **57** (1998) R2037.
17. K.W. Edmonds, R.P. Campion, K.-Y. Wang, A.C. Neumann, B.L. Gallagher, C.T. Foxon, and P.C. Main: J. Appl. Phys. **93** (2003) 6787.
18. S.U. Yuldashev, H.C. Jeon, H.S. Im, T.W. Kang, S.H. Lee, J.K. Furdyna, Phys. Rev. B **70** (2004) 193203.
19. D. Chiba, Y. Nishitani, F. Matsukura, H. Ohno, Appl. Phys. Lett. **90** (2007) 122503.
20. H. Ohno, H. Munekata, T. Penny, S. von Molnar, L.L. Chang, Phys. Rev. Lett. **68** (1992) 2664.
21. A. Oiwa, A. Endo, S. Katsumoto, Y. Iye, H. Ohno, Phys. Rev. B **59** (1999) 5826.
22. F. Matsukura, E. Abe, H. Ohno, J. Appl. Phys. **87** (2000) 6442.
23. T. Wojtowicz, W.L. Lim, X. Liu, G. Cywinski, M. Kutrowski, L.V. Titova, K. Yee, M. Dobrowolska, J.K. Furdyna, K.M. Yu, W. Walukiewicz, G.B. Kim, M. Cheon, X. Chen, S.M. Wang, H. Luo, I. Vurgaftman, J.R. Meyer, Physica E **20** (2004) 325.
24. Y. Lyanda-Geller, S.H. Chun, M.B. Salamon, P.M. Goldbart, P.D. Han, Y. Tomioka, A. Asamitsu, Y. Tokura, Phys. Rev. B **63** (2001) 184426.
25. P. Matl, N.P. Ong, Y.F. Yan, Y.W. Li, D. Studebaker, T. Baum, G. Doubinina, Phys. Rev. B **57** (1998) 10248.
26. Y. Onose, Y. Tokura, Phys. Rev. B **73** (2006) 174421.
27. R. Mathieu, A. Asamitsu, H. Yamada, K.S. Takahashi, M. Kawasaki, Z. Fang, N. Nagaosa, Y. Tokura, Phys. Rev. Lett. **93** (2004) 016602.
28. Y. Tomioka, T. Okuda, Y. Okimoto, R. Kumai, K.-I. Kobayashi, Y. Tokura, Phys. Rev. B **61** (2000) 422.
29. Y. Taguchi, Y. Oohara, H. Yoshizawa, N. Nagaosa, Y. Tokura, Science **291** (2001) 2573.
30. N. Manyala, Y. Sidis, J.F. Ditusa, G. Aeppli, D.P. Young, Z. Fisk, Nat. Mater. **3** (2004) 255.
31. Technical Raport (internal form), *extracted from the CEEX 2006 Project MATNANTECH C84/2006.*